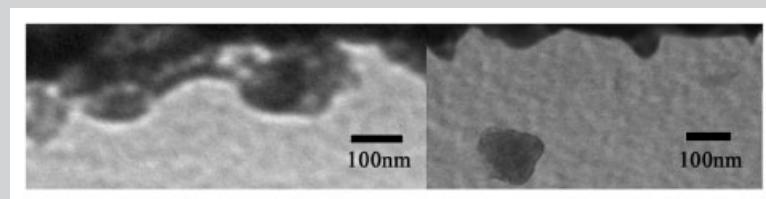


Summary: The effect of chain architecture of in situ formed copolymers on the interfacial morphology of reactive polymer blends was investigated. We found that the chain architectures of copolymers at the interface significantly affected the

reaction and interface roughness. Although the amount of in situ formed Y-shaped graft copolymers was smaller than that for diblock copolymers, the interface area generated by the former was larger than that generated by the latter.



Cross-sectional TEM images for the mid-sample reacted at 180 °C for different reaction times.

The Effect of Chain Architecture of In Situ Formed Copolymers on Interfacial Morphology of Reactive Polymer Blends

Hwang Yong Kim, Du Yeol Ryu,^a Unyong Jeong, Dong Han Kho, Jin Kon Kim*

National Creative Research Center for Block Copolymer Self-Assembly, Department of Chemical Engineering and Polymer Research Institute, Division of Electrical and Computer Engineering, Pohang University of Science & Technology, Kyungbuk 790-784, Korea
E-mail: jkkim@postech.ac.kr

Received: April 4, 2005; Revised: June 10, 2005; Accepted: July 4, 2005; DOI: 10.1002/marc.200500219

Keywords: chain architecture; interface morphology; microemulsion; reactive blend

Introduction

Reactive blending of two or more immiscible polymers with in situ reactive compatibilizers has been employed for developing new materials with desirable physical and mechanical properties and extensively investigated by many research groups.^[1–4] Two types of reactive compatibilizers have been investigated: one gives graft copolymers^[5–7] and the other gives diblock copolymers^[8–10], although the former has been usually adopted for commercial purposes. Then, a question is raised: which one has better compatibilization for two immiscible phases?

However, there has been little study on the effect of chain architecture of in situ formed copolymers on the compatibilization.^[11–13] Very recently, Jeon et al. showed that the

reaction kinetics for the formation of diblock copolymer generated from amine-terminated polystyrene (PS-NH₂) and phthalic anhydride end-functionalized poly(methyl methacrylate) (PMMA-eAn) was much faster than that of graft copolymer from PS-NH₂ and phthalic anhydride mid-functionalized PMMA (PMMA-mAn).^[11] But, the change in interfacial morphology for two different types of copolymers formed in situ near the interface has not been studied in detail.

Inoue et al.^[14–16] showed that the chain architecture of in situ formed copolymer affected the final morphology of polyamide/polysulfone (PA6/PSU) blend. Micelle formation, in particular, under the shear for graft copolymers formed from phthalic anhydride mid-functionalized PSU was different from that for diblock copolymers formed from end-functionalized PSU. However, due to the high polydispersities of these two reactive compatibilizers employed in ref.,^[14] the chain architectures of diblock and graft copolymers were difficult to determine.

^a Present address: Department of Chemical Engineering, Yonsei University, Seoul 120-749, Korea.

We previously showed that microemulsions were observed at only the PMMA phase near the interface for a reactive blend consisting of the end-functional monocarboxylated PS (PS-COOH) and glycidyl methacrylate functionalized PMMA (PMMA-GMA) having the functionality of ≈ 12.5 .^[17] The graft copolymers formed in this system were not well-defined, namely, as many as 12.5 PS chains might be grafted onto a single PMMA chain. Very recently, the micelles were observed for a reactive bilayer film generating diblock copolymers in situ at the interface.^[18,19] Thus, the effect of chain architecture (graft versus diblock) of in situ formed copolymers on reactive interfacial morphology and the formation of microemulsion is not clearly understood. This is because of tremendous efforts in synthesizing functional polymers with narrow molecular weights.

In this study, we investigated the effect of the chain architecture of in situ formed copolymers on interfacial morphology for reactive polymer blends. The reactive blend consisted of mono-functional glycidyl methacrylate terminated polystyrene (PS-GMA) and poly(methyl methacrylate) with carboxylate group (PMMA-COOH), where the positions of the carboxylate group are located at a third, the middle, and the end of the PMMA chain. The reaction between the carboxylate groups in PMMA-COOH and the epoxy groups in PS-GMA occurs easily at higher temperatures,^[20–25] giving in situ block (or graft) copolymers. We found that although the amount of in situ formed Y-shaped graft copolymers resulted from the mid-functionalized PMMA-COOH was smaller than that for diblock copolymers from the end-functionalized PMMA-COOH, the interface area generated by the former was larger than that generated by the latter. For the first time, we showed that only a reactive bilayer generating graft copolymers resulting from mid-functionalized polymer produced microemulsions near the reactive interface, but another reactive bilayer generating diblock copolymers did not.

Experimental Part

The GMA mono-functionalized PS was synthesized anionically in tetrahydrofuran (THF) containing excess dried LiCl at -78°C under purified argon using *s*-BuLi as an initiator. LiCl (high purity, Aldrich) was dried overnight at 170°C and then dissolved in dried THF. Styrene was first polymerized and then the GMA distilled from calcium hydride was added to the polystyrene anion and reacted for 1 h. The anion was terminated with degassed 2-propanol (Aldrich Chem. Co.). We found via ^1H NMR spectroscopy (Bruker, DRX500) that a single GMA was attached at the end of the PS chain, which was determined from the ratio of protons in CH_2 (≈ 4 ppm) located between ester and oxyranil groups in GMA to those in *s*-butyl (0.6–0.9 ppm) of the initiator. We also measured the functionality of GMA in PS-GMA by the nonaqueous back-titration method^[26,27]. PS-GMA was first dissolved in hot toluene, followed by the addition of trichloroacetic acid to the

solution. The reaction product was precipitated into ethyl acetate, and then filtered and washed. The filtrate was titrated with 0.1 N NaOH using phenolphthalein as an indicator. The functionality was determined to be ≈ 0.95 , which is essentially the same as that obtained from ^1H NMR.

Carboxylate functionalized PMMAs denoted as PMMA-COOH, where carboxylic acid functional groups are located at one-third of the total length of PMMA chain, and the middle and the end of PMMA chain, were synthesized by the sequential, anionic polymerization of MMA and *tert*-butyl acrylate (*t*-BA) in THF at -78°C in the presence of LiCl under purified Ar environment. The initiator for PMMA-COOH was prepared by the addition of *s*-BuLi to 1,1-diphenylethylene (1:1 mole ratio) in the purified THF solution for 4 h. MMA monomer was first polymerized in THF solution with *s*-BuLi. For PMMAs with COOH at the third and the middle positions, *t*-BA was added and reacted for 4 h. Then, MMA monomer was added and reacted again for 4 h. For the PMMA with COOH at the end of the PMMA chain, *t*-BA was added after the complete polymerization of MMA. The amount of *t*-BA in PMMA chain was determined from the ratio of protons in *tert*-butyl group (1.3–1.5 ppm) to those in 1,1-diphenylethylene (7.0–7.3 ppm) of the initiator.

All PMMAs with *t*-BA were hydrolyzed into carboxylic acid (COOH) according to the method given in ref.^[28] We found that all *t*-BA were transformed to COOH, which was confirmed by the fact that the NMR peak corresponding to *t*-BA disappeared completely. The number- and weight-average molecular weights (\bar{M}_n and \bar{M}_w) of all polymers were measured by gel permeation chromatography (GPC: Waters Co., 600F) with a multi-angle laser light scattering detector (MALLS). The characteristics of all polymers employed in this study are given in Table 1. Hereafter, we refer to the end-sample, the 1/3-sample and the mid-sample to copolymers generated from end-, 1/3-, and mid-positioned carboxylate functionalized PMMA reacted with PS-GMA.

To measure the extent of the reaction between three PMMA-COOHs and PS-GMA at molten state, the bilayer films consisting of these two polymers having thickness of 80 nm for each layer (thus total film thickness of 160 nm) were spin-coated and reacted at 180°C for two different reaction times (8 and 32 h). After the bilayer film was dissolved into THF, GPC trace was obtained by GPC-MALLS. Since there was no peak observed in the GPC trace corresponding to the molecular weight resulting from two (or more) PS chains grafted onto PMMA chains, we concluded that only a single PS chain reacted with PMMA chains. From the peak deconvolution of the GPC trace, the amount of the end-sample reacted for 8 h was approximately four times larger than that of the graft copolymer generated from mid-sample, while that of the graft

Table 1. Characteristics of polymers employed in this study.

Samples	\bar{M}_n kg · mol ⁻¹	\bar{M}_w/\bar{M}_n	Functionality
PS-GMA	50.1	1.04	1
PMMA-COOH (end)	29.5	1.05	1.8
PMMA-COOH (mid)	30.2	1.05	1.8
PMMA-COOH (1/3)	30.1	1.05	1.8

copolymer generated from 1/3-sample was ≈ 2.5 times larger than that of the mid-sample. After 32 h reaction, the amount of the end-sample was ≈ 1.8 times larger than that of the mid-sample. The amount of the end-sample did not increase after 8 h reaction at 180 °C. It is noted that when the total film thickness was decreased to 60 nm, the amount of the end-sample after 32 h reaction was ≈ 2.2 times larger than that of the mid-sample. This is because the total film thickness is smaller than the rms roughness (≈ 80 nm) of the mid-sample at 32 h reaction; thus this small film thickness could not accommodate all of the graft copolymers. But, the amount of the mid-sample reacted for 32 h did not change with film thickness as long as the total bilayer film thickness was larger than 160 nm.

A bilayer film consisting of PS-GMA and PMMA-COOH was prepared by sequential spin-casting onto a silicon wafer. The thickness of each layer was ≈ 300 nm measured by a spectroscopic ellipsometer (J.A. Woollam Co.; M-2000V) and atomic force microscopy (AFM: Digital Instrument; D3000) with silicon nitride tips on cantilevers (Nanoprobe) in the tapping mode. The reaction was conducted at 180 °C under nitrogen environment for various times up to 50 h. We found that there was no thermal degradation of PMMA and PS after the reaction. After the reaction, unreacted PS-GMA layer was completely removed by selective solvent of cyclohexane at 40 °C for 1 h, which was confirmed by the fact that the peak in the GPC trace corresponding to PS-GMA disappeared when the remaining film was dissolved into THF. The interface was observed by AFM, and rms roughness was calculated by the software (Nanoscope) provided by Digital Instrument. The cross-sectional morphology near the interface as well as the presence of microemulsions or micelles was observed by transmission electron microscopy (TEM: Hitachi; 7600) operating at 120 kV. The samples for TEM observation were prepared by the same method as that in ref.^[29]

Results and Discussion

AFM height images for three samples after being reacted at 180 °C for 32 h are given in Figure 1. The thickness of each layer was ≈ 300 nm. The rms roughness of the end- and 1/3-samples was 20 and 40 nm, respectively, whereas that for the mid-sample was 85 nm. Based on AFM results for all samples reacted at various reaction times at 180 °C, the change of rms roughness with reaction time is given in Figure 2. At reaction times less than 8 h, the rms roughness of all three samples was almost the same. However, the rms roughness of the end-sample did not increase with further reaction time.

Now, we consider the rms roughness at reaction times less than 8 h. It is noted that the total interfacial area (A_t) is expressed by the amount of in situ formed copolymers (or total number of chains at the interface) multiplied by the interfacial area (A_j) per single copolymer chain. Also, A_t depends on only two parameters: rms roughness and wavelength (λ) of the roughness. But, it is not linearly proportional to the rms roughness even for the same λ . We found that λ obtained from AFM images (see Figure 1) for both Y-shaped graft and diblock copolymers was almost the same

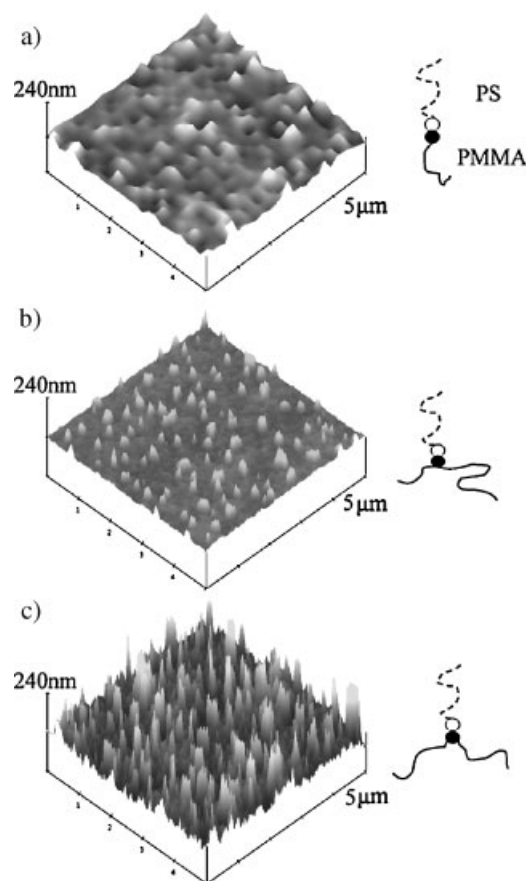


Figure 1. AFM height images and chain architectures for three samples reacted at 180 °C for 32 h: (a) the end-sample with an rms roughness of 20 nm, (b) 1/3-sample with an rms roughness of 40 nm, and (c) the mid-sample with an rms roughness of 85 nm.

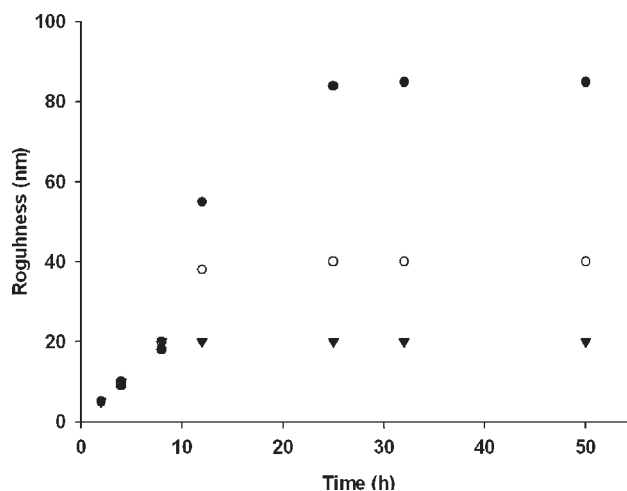


Figure 2. The values of rms roughness with reaction time at 180 °C for three samples: the end-sample (▼), 1/3-sample (○), and the mid-sample (●).

(≈ 200 nm). Since the rms roughness of the mid-sample was almost the same as that of the end-sample at reaction times less than 8 h, A_t for these two samples should be similar. However, the amount of the former generated at the interface for 8 h reaction was about one-fourth of the latter (see Experimental Part). This indicates that A_j for graft copolymer should be larger than that for diblock copolymer. The larger A_j of graft copolymers compared with diblock copolymer was due to Y-shaped graft copolymers where the steric hindrance between two heads of Y-shape is larger than that of diblock copolymer.

The A_j is also calculated by assuming that the interface is densely covered by a single layer of both copolymers.^[30–32]

$$A_j = \frac{M_i}{N_{AV}\rho_i(L_i/2)} \quad (1)$$

where M_i , L_i , and ρ_i are the molecular weight, the layer thickness, and the density of i -block, and N_{AV} is Avogadro's number. Although there has been no report for A_j for Y-shaped PS-PMMA graft copolymer, the value of L_i for Y-shaped graft PS-polyisoprene (PI) copolymer is available in the literature.^[32] When this value is compared with that of PS-*block*-PI copolymer, the ratio of A_j between Y-shaped graft copolymer and diblock copolymer is calculated to be 1.7, smaller than ≈ 4 , which was obtained from the reaction kinetics. This discrepancy suggests that a dense packing for Y-shaped graft copolymers was not attained at the interface for 8 h reaction, which makes A_j larger than that for densely packed Y-shaped copolymers.

Now, we consider reaction times longer than 25 h, where rms roughness of the mid-sample (85 nm) is much larger than that (≈ 20 nm) of the end-sample. One might have a question that the amount of Y-shaped copolymer at longer reaction times would be larger than that of diblock copolymer. From the relationship between the interface roughness and A_t , the ratio of A_t between the mid-sample and the end-sample is calculated to be 1.4.^[33] Since the amount of the mid-sample reacted for 32 h was about half of that of the end-sample, we concluded that the A_j of the mid-sample was still larger than that of the end-sample even for 32 h reaction. Namely, the densely packed Y-shaped chains would not be achieved even at 32 h reaction.

Figure 3(a) and (b) give cross-sectional TEM images for the end- and 1/3-samples after 32 h reaction at 180 °C. The interfacial roughness of the end- and 1/3-samples is well consistent with the rms values obtained from AFM images. Micelles or microemulsions were not observed. Figure 3(c–e) show TEM images for the mid-sample reacted at three different times (25, 32, and 50 h). More roughened interfaces were observed for the mid-sample reacted for 25 h compared with other two samples. Namely, most parts of the sample remained pinch-off, but microemulsions were not observed in this sample. Interestingly, when the sample was reacted for 32 h, microemulsions were clearly seen in some areas. It is noted, however, that most interfaces still

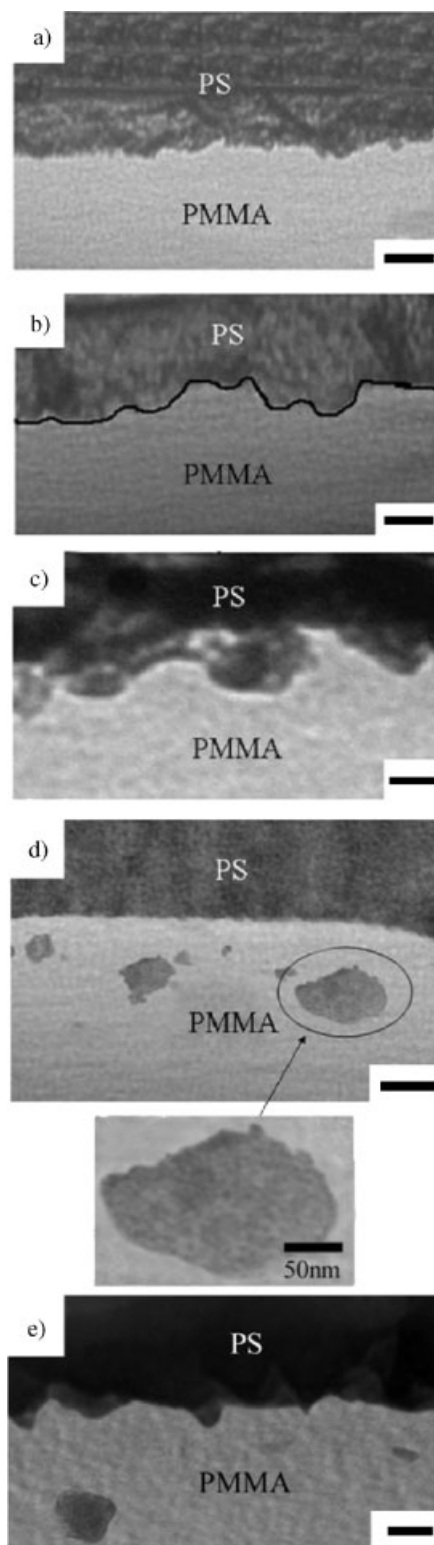


Figure 3. Cross-sectional TEM images for (a) the end-sample and (b) 1/3-sample reacted at 180 °C for 32 h. (c–e) Cross-sectional TEM images for the mid-sample reacted at 180 °C for three different reaction times [(c) 25 h (d) 32 h, and (e) 50 h]. Dark regions represent PS phase stained with the RuO_4 . The length of all scale bars is 100 nm except magnified image of microemulsion.

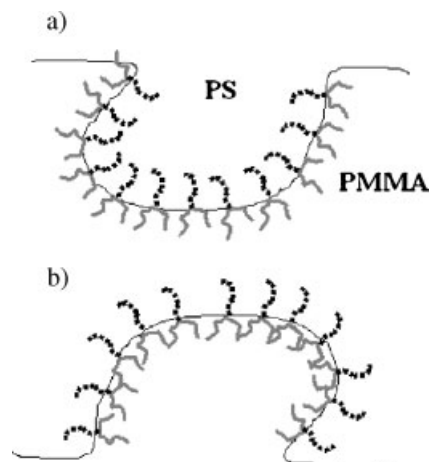


Figure 4. Schematic for different locations of two branches of Y-shaped graft copolymer near the interface. (a) Two branches of Y-shaped graft copolymers are located outer the curvature and (b) two branches are located inside the curvature.

remained pinch-offs in TEM image (not shown) similar to Figure 3(c); thus the rms roughness would be quite large at 32 h reaction, consistent with AFM images. To observe change of the rather flat interfaces near the microemulsions, as shown in Figure 3(d), with further reaction time, a long reaction (50 h) was carried out, and the TEM image for this case is given in Figure 3(e). Comparing Figure 3(d) and (e), the rather flat interface near which microemulsions were observed became corrugated again with increasing reaction time. This is because additional large reaction time is required for a flat interface to be corrugated again. We also noted that the protrusion direction of the pinch-offs was toward PMMA phase, and microemulsions were also observed in the PMMA phase, not in the PS phase. This asymmetric phenomenon was also observed in our previous study.^[17] The reason why the microemulsions were observed in only PMMA phase could be explained in Figure 4. An interface where two branches of Y-shaped copolymer are located outside of the curvature [Figure 4(a)] is more stable than another interface given in Figure 4(b). This is because two branches need more space to avoid steric hindrance. This result would be consistent with previous results where chain architecture of copolymers (diblock vs. graft) affected the stability of micelles significantly.^[34,35] For instance, micelles formed by graft copolymer, whose head part is located inside the curvature, are less stable than that by diblock copolymer.^[34] On the other hand, when the head direction of graft copolymer becomes reverse, micelles formed by graft copolymers are more stable than that by diblock copolymer.^[35] Also, the degree of the interfacial tension reduction is varied depending upon the location of the head part of graft copolymer.^[36]

As described previously, the amount of in situ formed diblock copolymer was larger than that of graft copolymer. This led us to consider that the main difference in the

interfacial roughness was the chain architecture, not the amount of in situ formed copolymer. Finally, for the 1/3-sample, the shorter chain in two branches of Y-shaped copolymers is not enough longer to stabilize the curvature, since the molecular weight ($\approx 10\,000$) of the shorter chain is close to the entanglement molecular weight ($\approx 10\,000$)^[37] of PMMA. Thus, the 1/3-sample showed similar interfacial morphology development to the end-sample, not the mid-sample.

The result for the end-sample might be contrasted to that given in the literatures,^[8,10,18,19] where highly roughened interfaces and micelles without containing homopolymers were observed in end-functionalized PS-NH₂ and PMMA-anh reactive blend under static reaction without shearing. This discrepancy might be due to different reaction kinetics, final conversion, and molecular weight of reactive polymers. It is noted that the reaction kinetics (and conversion) between acid and epoxy employed in this study are much slower (and lower) than those between anhydride and amine. The exact explanation would be a subject for future investigation.

Conclusion

We have shown that the chain architecture of in situ formed copolymers significantly affected the reaction kinetics and interfacial morphology of reactive polymer blends. To control the chain architecture of in situ formed copolymers, three different PMMA-COOHs were synthesized anionically. We found that the amount of in situ formed Y-shaped graft copolymer was smaller than that for diblock copolymer. However, the interfacial roughness generated from the former was larger than that generated from the latter. Furthermore, only the middle sample exhibited microemulsions at the PMMA phase. This is because two branches in Y-shaped copolymer should be located at the outside of the curved interface (namely, the PMMA phase) to accommodate more spaces.

Acknowledgements: This work was supported by the *National Creative Research Initiative Program* supported by KOSEF.

- [1] F. Ide, A. Hasegawa, *J. Appl. Polym. Sci.* **1974**, *18*, 963.
- [2] J. S. Schulze, B. Moon, T. P. Lodge, C. W. Macosko, *Macromolecules* **2001**, *34*, 200.
- [3] Z. Yin, C. Koulic, C. Pagnouille, R. Jérôme, *Macromol. Chem. Phys.* **2002**, *203*, 2021.
- [4] H. T. Oyama, T. Inoue, *Macromolecules* **2001**, *34*, 3331.
- [5] K. Dedecker, G. Groeninckx, T. Inoue, *Polymer* **1998**, *39*, 4993.
- [6] K. Dedecker, G. Groeninckx, *Macromolecules* **1999**, *32*, 2472.

- [7] D. Vlassopoulos, M. Pitsikalais, N. Hadjicristidis, *Macromolecules* **2002**, *33*, 2000.
- [8] S. P. Lyu, J. J. Cernohous, F. S. Bates, C. W. Macosko, *Macromolecules* **1999**, *32*, 106.
- [9] J. Jiao, E. J. Kramer, S. d. Vos, M. Möller, C. Koning, *Macromolecules* **1999**, *32*, 6261.
- [10] Z. Yin, C. Koulic, C. Pagnouille, R. Jérôme, *Langmuir* **2003**, *19*, 453.
- [11] H. K. Jeon, C. W. Macosko, B. Moon, T. R. Hoye, Z. Yin, *Macromolecules* **2004**, *37*, 2563.
- [12] Z. Yin, C. Koulic, C. Pagnouille, R. Jérôme, *Macromol. Symp.* **2003**, *198*, 197.
- [13] R. Adhikari, G. H. Michler, *Prog. Polym. Sci.* **2004**, *29*, 949.
- [14] P. Charoensirisomboon, T. Chiba, S. I. Solomko, T. Inoue, M. Weber, *Polymer* **1999**, *40*, 6803.
- [15] P. Charoensirisomboon, T. Inoue, M. Weber, *Polymer* **2000**, *41*, 4483.
- [16] P. Charoensirisomboon, T. Inoue, M. Weber, *Polymer* **2000**, *41*, 6907.
- [17] H. Y. Kim, U. Jeong, J. K. Kim, *Macromolecules* **2003**, *36*, 1594.
- [18] B. J. Kim, H. Kang, K. Char, K. Katsov, G. H. Fredrickson, E. J. Kramer, *Macromolecules* **2005**, *38*, 6106.
- [19] J. Zhang, T. P. Lodge, C. W. Macosko, *Macromolecules* **2005**, *38*, 6568.
- [20] J. K. Kim, H. Lee, *Polymer* **1996**, *37*, 305.
- [21] H. K. Jeon, J. K. Kim, *Macromolecules* **1998**, *31*, 9273.
- [22] [22a] H. K. Jeon, J. K. Kim, *Polymer* **1998**, *39*, 6227; [22b] H. K. Jeon, J. K. Kim, *Korea Polym. J.* **1999**, *7*, 124.
- [23] H. K. Jeon, H. T. O. Oyama, J. K. Kim, *Polymer* **2001**, *42*, 3259.
- [24] H. K. Jeon, J. K. Kim, *Macromolecules* **2000**, *33*, 8200.
- [25] C. A. Orr, J. J. Cernohous, P. Guegan, A. Hirao, H. K. Jeon, C. W. Macosko, *Polymer* **2001**, *42*, 8171.
- [26] P. Citovicky, V. Chrastova, *Plast. Kautsch.* **1984**, *31*, 374.
- [27] H. Huang, N. C. Liu, *J. Appl. Polym. Sci.* **1998**, *67*, 1957.
- [28] J. P. Hautekeer, S. K. Varshney, R. Fayt, C. Jacobs, R. Jérôme, Ph. Teyssié, *Macromolecules* **1990**, *23*, 3893.
- [29] D. H. Kho, S. H. Chae, U. Jeong, H. Y. Kim, J. K. Kim, *Macromolecules* **2005**, *38*, 3820.
- [30] H. Tanaka, H. Hasegawa, T. Hashimoto, *Macromolecules* **1991**, *24*, 240.
- [31] D. J. Pochan, S. P. Gido, S. Pispas, J. W. Mays, *Macromolecules* **1996**, *29*, 5099.
- [32] K. I. Winey, E. L. Thomas, L. J. Fetters, *Macromolecules* **1991**, *24*, 6182.
- [33] H. Y. Kim, J. K. Kim, unpublished.
- [34] J. Yun, R. Faust, L. S. Szilágyi, S. Kéki, M. Zsuga, *Macromolecules* **2003**, *36*, 1717.
- [35] T. K. Bronich, T. Cherry, S. V. Vinogradov, A. Eisenberg, V. A. Kabanov, A. V. Kabanov, *Langmuir* **1998**, *14*, 6101.
- [36] H. Retsos, H. Anastasiadis, S. Pispas, J. W. Mays, N. Hadjichristidis, *Macromolecules* **2004**, *37*, 524.
- [37] L. J. Fetters, D. J. Lohse, D. Richter, T. A. Witten, A. Zirkel, *Macromolecules* **1994**, *27*, 4639.